13th International Conference Series on
Laser-light and Interactions with Particles
Optical Particle Characterization follow-up !
August 21-26th, 2022, Warsaw, Poland

INSTYTUT FIZYKI POLSKIEJ AKADEMII NAUK

Glare Points and Near-Zone Sagittal Caustic for Scattering of a Plane Wave by a Spherical or Spheroidal Bubble Floating in Air

James LOCK [1,*] and Markus SELMKE [2]

[1] Physics Department, Cleveland State University, Cleveland, OH 44115, USA
[2] Fraunhofer Institute for Applied Optics and Precision Engineering IOF, Center of Excellence in Photonics, Albert-Einstein Str. 7, 07745 Jena, Germany

**Corresponding author j.lock@csuohio.edu*

Abstract

We examine various features of scattering of a plane wave by a spherical or spheroidal bubble floating in air. We interpret the pattern of glare points observed on the far-zone image of the bubble, and the near-zone sagittal caustic of light scattered following one internal reflection. We find the symmetry inherent in these features for a spherical bubble is broken as the bubble is deformed into a shape of lower symmetry.

1 Introduction

We consider a linearly polarized monochromatic plane wave of light of wavelength λ incident on a nonabsorbing spherical bubble floating in air. The bubble has inner radius a and film thickness d<<a, with a~O(cm), and d~O(μm). The bubble film has real refractive index n, and both the region exterior to the bubble film and the interior of the bubble have unit refractive index. Rays are transmitted into the bubble, and internally reflect p-1 times from the bubble film before being transmitted out.

When an observer stands in the far-zone at a scattering angle Θ_{scatt} in the backward hemisphere and looks at a floating bubble illuminated by sunlight, he sees a sequence of glare points to each side of center that appear to lie on the image of the bubble. The observed glare points lie in the plane containing the bubble's center, the observer, and the light source. They are progressively closer together and become progressively dimmer as they approach the edge of the image of the bubble. Photographs illustrating this effect and taken by one of the authors (M.S.) are reproduced here as Figs.1,2. The location, intensity, and color of the glare points as viewed by the observer depend on the scattering angle and far-zone intensity of the light scattered by the bubble.

Since a spherical floating bubble is a surface of revolution with respect to the propagation direction of the incident plane wave, the two branches of the near-zone caustic of the scattered rays for each value of p can straightforwardly be determined. The tangential caustic is obtained by finding the locus of the intersection points of adjacent converging rays that are confined to a single plane. The tangential caustic for each value of p lies entirely inside the bubble and is not considered further here. The sagittal caustic is obtained by determining the locus the positions where azimuthal families of rays making p-1 internal reflections cross the z axis. The sagittal caustics on the positive z axis outside the bubble surface decrease very quickly in intensity as a function of z. As a result, in order to view the sagittal caustic, a viewing screen must be placed behind the bubble close to the floating bubble surface. This is also illustrated in Fig.1.

2 Floating Bubble Ray Theory

The floating bubble geometry is a special case of a coated sphere. In the short wavelength limit, $2\pi a/\lambda$~10^5 we use a simplified version of coated sphere ray theory [1]. The usual reflection law is assumed to hold for a ray internally or externally reflected by the thin bubble film. We also assume that rays are transmitted through the thin bubble film without deflection. We model the intensity of the reflected and transmitted parts of the incident broadband spectrum at each interaction with the surface in three stages. First, the intensity Fresnel coefficient for coherent monochromatic light for a single flat interface between the bubble film and the air outside or inside the bubble is denoted by R for either the transverse electric or transverse magnetic polarization.

We are interested in the simplifications that occur for near-grazing rays, where the angle of incidence θ_i^0 is near 90°. We define the small quantity σ<<1 for these rays by

$$\sigma \equiv \cos(\theta_i^0)\ . \qquad (1)$$

Then for rays with near-grazing incidence,

$$R = 1 - \alpha\sigma + O(\sigma^2)\ , \qquad (2)$$

where α is a polarization-dependent constant of proportionality. Second, one sums the infinite series of successive coherent interactions of a ray with the outer and inner surfaces of the film. The resulting coherent intensity Fresnel coefficient for transmission through the film is T_{film}^{coh} and the resulting coherent intensity Fresnel coefficient for reflection by the film is R_{film}^{coh}. Third, the floating bubble is illuminated by broadband visible sunlight. Thus, the monochromatic intensity Fresnel coefficients must be integrated over both the source spectrum and the sensitivity of the eye of the observer for $0.4\mu m \approx \lambda_{min} \leq \lambda \leq \lambda_{max} \approx 0.7\mu m$. We make the simplifying assumptions that (i), both the source spectrum and the sensitivity of the eye of the observer are flat between λ_{min} and λ_{max}, and (ii) the film thickness is sufficiently large that the phase ε of the interference between successive paths in the film varies by at least O(π) in this wavelength interval. The spectrum-averaged intensity Fresnel coefficient for internal or external reflection of an incident ray by the thin film is then approximated by

$$(R_{film})^{ave} \approx (1/\pi) \int_0^\pi d\varepsilon\, R_{film}^{coh} \ , \qquad (3)$$

and the spectrum-averaged intensity coefficient for transmission into the bubble interior and transmission back out following p-1 internal reflections is approximated by

$$(T_{film}\, R_{film}^{p-1}\, T_{film})^{ave} \approx (1/\pi) \int_0^\pi d\varepsilon\, T_{film}^{coh}\, (R_{film}^{coh})^{p-1} T_{coh}^{film} \,. \qquad (4)$$

Assuming that the incident wave propagates in the +z direction, we let $\Theta_p(\theta_i^0)$ be the deflection angle of the incident ray whose angle of incidence is θ_i^0 at the outer surface of the bubble film, and that makes p-1 internal reflections before exiting. for p=0 external reflection we have

$$\Theta_0(\theta_i^0) = \pi + 2\theta_i^0 \,, \qquad (5)$$

and for $p \geq 2$ we have

$$\Theta_p(\theta_i^0) = (p-1)(\pi - 2\theta_i^0) \,. \qquad (6)$$

We obtain the far-zone intensity of the light scattered by a spherical floating bubble using flux conservation. We assume that successive interactions of a ray with the bubble film at different locations on the floating bubble are incoherent with respect to each other. This assumption is valid because the path length of the ray between these interactions is comparable to the bubble radius, typically ~O(cm) or ~O(mm) for near-grazing incident rays, while the bubble film thickness and the longitudinal coherence length of sunlight are ~O(μm). The far-zone scattered intensity for rays making p-1 internal reflections at the spherical bubble film for $p \geq 2$ is

$$I_p^{scatt}(\Theta_{scatt}) = I_{inc}(a/R_{vs})^2[1/2(p-1)][\sin(\theta_i^0) \cos(\theta_i^0)/\sin(\Theta_{scatt})] \times [T_{film}(\theta_i^0)\, R_{film}^{p-1}(\theta_i^0)\, T_{film}(\theta_i^0)]^{ave} \,, \qquad (7)$$

where I_{inc} is the intensity of the incoming ray, and R_{vs} is the distance from the center of the floating bubble to the far-zone viewing screen, and the scattering angle Θ_{scatt} associated with the deflection angle Θ_p lies within the interval $0° \leq \Theta_{scatt} \leq 180°$. The polarization of the spectrum-averaged intensity coefficients depends on the plane of incidence of the ray. Similarly, the externally reflected contribution to the scattered intensity is

$$I_0^{scatt}(\Theta_{scatt}) = I_{inc}\, (a/2R_{vs})^2\, [R_{film}(\theta_i^0)]^{ave} \,. \qquad (8)$$

Since the directly transmitted light is forward-propagating, it is combined with diffraction to obtain $I_1^{scatt}(\Theta_{scatt})$ in the near-forward direction.

3 Reflection Glare Points of a Spherical Floating Bubble

When the far-zone observer either focuses his eyes on the bubble or photographs it, he records the magnitude-squared of the Fourier transform of the far-zone scattered intensity that is windowed in an interval centered on Θ_{scatt}, whose width is determined by the eye's or camera's aperture [2]. Let the coordinate χ extend from edge to edge, $-L \leq \chi \leq L$, on the equator of the image of the bubble recorded by the observer. The location of the center of the $M \geq 0$ glare spot for p-1 internal reflections of the ray from the bubble film with $p \geq 2$ is then [2,3]

$$\chi_{p,M} = L \cos\{(\Theta_{scatt} + 2\pi M)/[2(p-1)]\} \,, \qquad (9)$$

where the range of allowed values of M are

$$0 \leq (\Theta_{scatt} + 2\pi M)/[2(p-1)] \leq \pi \,. \qquad (10)$$

The center of the external reflection glare point for $(p,M)=(0,0)$ occurs at

$$\chi_{0,0} = -L \cos(\Theta_{scatt}/2) \qquad (11)$$

corresponding to the angle of incidence $-\theta_i^0$. The center of the one-internal-reflection glare point for $(p,M)=(2,0)$ occurs at

$$\chi_{2,0} = L \cos(\Theta_{scatt}/2) \qquad (12)$$

corresponding to the angle of incidence of $+\theta_i^0$. These two glare points are symmetrically located on the equator of the image of the spherical floating bubble, and with Θ_{scatt} in the backward hemisphere, are the brightest glare spots observed. Their intensity ratio is

$$I_{2,0}^{glare} \,/\, I_{0,0}^{glare} = (1-R)(1-R+R^2)/(1+R^4) \,. \qquad (13)$$

If the bubble film has n=1.333, the glare point intensity ratio decreases from 0.886 to zero as the observer moves from Θ_{scatt}=180° where θ_i^0=±0°, to Θ_{scatt}=0° where θ_i^0=±90°.

When the observer is in the backward hemisphere, the sequence of closely-spaced glare points seen near the edge of the bubble, and which are due to rays having near-grazing incidence, become progressively dimmer as $\chi \rightarrow |L|$ because

$$I_{p,M}^{glare} \propto \sigma^2 \,. \qquad (14)$$

From top to bottom in Fig.1, the visible glare points are $7 \geq p \geq 2, M=0$, then $p=0, M=0$, then $3 \leq p \leq 8, M=p-2$. The scattering angle of the observer is $\Theta_{scatt} \approx 133°$.

4 Sagittal Caustic of a Spherical Floating Bubble

The parametric equation of the sagittal caustic as a function of p and $0 \leq |\theta_i^0| \leq 90°$ is

$$z_s = (-1)^p\, a \sin(|\theta_i^0|) \,/\, \sin[2(p-1)|\theta_i^0|] \qquad (15a)$$

$$\rho_s = 0 \,. \qquad (15b)$$

Each value of p contributes its own sagittal caustic, and all the sagittal caustics lie on top of each other on the z axis. The p=2 sagittal caustic lies inside the bubble for $0° \leq \theta_i^0 \leq 60°$, and outside the bubble on the +z axis for $60° < \theta_i^0 \leq 90°$. Its location on the z axis as a function of σ in the near-grazing incidence regime is

$$z_s \approx a/2\sigma + O(\sigma^2), \qquad (16)$$

and its relative intensity, [4]

$$I_{rel} \approx I_{inc}\, (1/128)\, \alpha a^5/z^4 \,, \qquad (17)$$

falls off very rapidly as a function of z.

5 Reflection Glare Points of a Spheroidal Floating Bubble

As a floating bubble is launched, it undergoes transient shape oscillations that quickly damp out to a final spherical shape. The dominant transient shape oscillation is a quadrupole deformation between an oblate and prolate spheroid, given by

$x_s^2/a^2 + y_s^2/a^2 + z_s^2/b^2 = 1$ (18)

in the spheroid coordinate system. The spheroidal bubble is arbitrarily orientated with respect to a far-zone observer in the $(\Theta_{scatt},\Phi_{scatt})$ scattering direction whose viewing screen plane is normal to this direction, and has axes x_{vs} and y_{vs}. The path of the externally reflected ray and the one-internal-reflection ray can be traced through the bubble [5]. It is found that these two reflection glare points continue to be located at equal distances in opposite directions with respect to the center of the elliptical image of the spheroid on the viewing screen. But the line joining the two glare points is now rotated by the angle Ω with respect to the x_{vs} axis. For side-on incidence of the plane wave this angle simplifies to

$\tan(\Omega) \approx [(a^2/b^2) - 1] \sin(\Phi_{scatt}) \cos(\Phi_{scatt})$. (19)

The related 4° rotation of the dominant glare points with respect to the higher-order glare points is evident in Fig.2. The semimajor and semi-minor axes of the elliptical image of the spheroid are also rotated by the angle Γ with respect to the x_{vs} and y_{vs} axes. For side-on incidence, this angle simplifies to

$\tan(2\Gamma) = -\cos(\Theta_{scatt}) \sin(2\Phi_{scatt})$
$/ [\cos(2\Phi_{scatt}) - \sin^2(\Theta_{scatt}) \cos^2(\Phi_{scatt})]$. (20)

6 Sagittal Caustic of a Spheroidal Floating Bubble

The transient spheroidal shape of the bubble also spoils the point-focusing of the near-zone sagittal caustic observed on a viewing screen behind the bubble in the Θ_{scatt}=0° direction. The formula for the exact shape of the one-internal-reflection sagittal caustic can be determined using the wavefront propagation method [6] since the spheroid still possesses circular symmetry about its axis. For side-on incidence of the plane wave, we are interested in the shape of the sagittal caustic in the vicinity of the positive z axis outside the bubble for one-internal-reflection rays that approach the spheroid with near-grazing incidence. In this limit the shape of the resulting caustic can be expanded in terms of powers of σ. To first order, this gives the four-cusped astroid caustic,

$(x_{vs})^{2/3} + [(b/a)y_{vs}]^{2/3} = a^{2/3} [1 - (b^2/a^2)]^{2/3}$, (21)

seen in Fig.2. If a threefold-symmetric harmonic shape distortion of the spheroid shape were present in addition to the dominant twofold-symmetric quadrupole distortion, one of the astroid cusps expands into a three-cusped butterfly caustic [7]. If a fourfold-symmetric hormonic shape distortion was additionally present instead, two opposing cusps of the astroid expand into butterfly caustics. One of the authors (M.S.) has observed and photographed these higher-order near-zone sagittal caustics behind the bubble.

7 References

[1] Princen H.M., Mason S.G., Optical interference in curved soap films, J. Coll. Sci. 20:453-63 (1965).

[2] Lock J.A., Theory of the observations made of high-order rainbows from a single water droplet, Appl. Opt. 26:5291-8 (1987)

[3] Van de Hulst H.C., Wang R.T., Glare points, Appl. Opt. 30:4755-63 (1991)

[4] Burkhard D.G., Shealy D.L., Formula for the density of tangent rays over a caustic surface, Appl. Opt. 21:3299-306 (1982)

[5] Lock J.A., Ray scattering by an arbitrarily oriented spheroid. I. Diffraction and specular reflection, Appl. Opt. 35:500-14 (1996)

[6] Marston P.L., Geometrical and catastrophe methods in scattering, Phys. Acous. 21:1-234 (1992), section 2.8

[7] Berry M.V., Waves and Thom's theorem, Adv. Phys. 25:1-26 (1976)

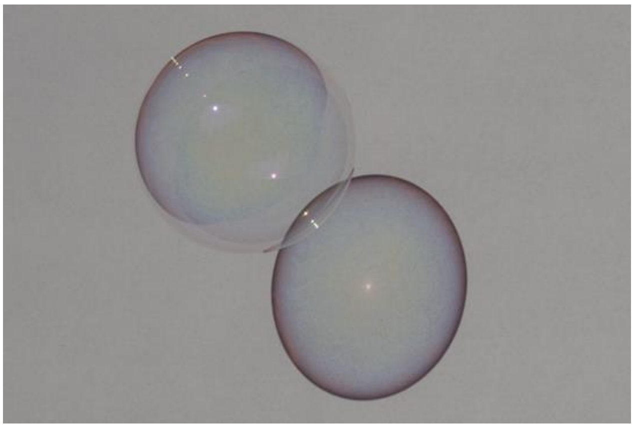

Figure 1 *Glare points on the surface of a spherical floating bubble, and a cross section through the near-zone sagittal axial spike caustic on a viewing screen behind the bubble.*

Figure 2 *Glare points on the surface of a spheroidal floating bubble, and a cross section through the near-zone sagittal astroid caustic on a viewing screen behind the bubble.*